ARPHA Proceedings

Proceedings CAUSummit 2024, 0335-0344
doi: 10.3897/ap.7.e0335

World Summit: Civil Engineering-Architecture-Urban Planning Congress

Amplitude Scaling for Ground Motion Modification Using Firefly Algorithm

Richard Frans[1, a)], Yoyong Arfiadi[2], Ade Lisantono[2]

[1] *Civil Engineering Department, Universitas Atma Jaya Makassar, Makassar, 90224, Indonesia*
[2] *Civil Engineering Department, Universitas Atma Jaya Yogyakarta, Yogyakarta, 55281, Indonesia*

[a)] Corresponding author: richardfrans.rf@gmail.com

Abstract. One step in the nonlinear response time history analysis technique used in designing earthquake-resistant structural buildings is the selection and modification of ground motion. In Indonesia, this clause is found in SNI 8899:2020, which deals with procedures for selecting and modifying surface ground motion for designing earthquake-resistant buildings. This research will discuss ground motion modification based on historical earthquake recordings and spectrum targets. Amplitude scaling and spectral matching are the two common techniques utilized in ground motion modification. Amplitude scaling is a straightforward technique that lowers computing costs. The firefly algorithm will be used in this study to approximate the scale factor in the amplitude scaling method. Eleven sets of earthquake recordings were utilized, following the examples found in SNI 8899:2020. The objective function is taken as reducing the limit ratio between the target spectrum and the average spectrum of recorded earthquakes. A comparison will be made between the scale factor found in SNI 8899:2020 and the scale factor obtained by the firefly method. The scale factors in the periods $0.2T1_B - 2T1_A$ and $0.2T1_B - 1.5T1_A$ are the two that will be compared.

Keywords: Amplitude scaling, ground motion modification, firefly algorithm

Published by CAUSummit and peer-reviewed under the responsibility of "World Summit: Civil Engineering-Architecture-Urban Planning Congress - CAUSummit-2024".

INTRODUCTION

Nonlinear dynamic analysis is a compelling instrument for determining seismic capacity and EDPs of structures and infrastructures by utilizing the set of ground motion records as input [1]. Any ground motion to be used in dynamic analysis must be scaled to match or even exceed the target spectrum [2,3]. There are two suitable ground motion modification methods: amplitude scaling (wherein the ground motion is uniformly scaled so that the resulting spectrum matches the amplitude of the design spectrum at the structural fundamental period) and spectrum matching [4]. These two methods have been applied in many research studies to find the performance of the building [5-7]. However, this study does not address the building's performance after obtaining the changed response spectrum. This study aims to determine the scale factors in the amplitude scaling method at specific intervals, following the guidelines outlined in SNI 8899:2020. SNI 8899:2020 was utilized as a seismic code reference for the purpose of adjusting surface ground motion. According to SNI 8899:2020, two specific time intervals are used as a reference for scaling.

These intervals are $0.2T1_B - 2T1_A$ and $0.2T1_B - 1.5T1_A$. $T1_B$ represents the smallest fundamental vibration period for the main horizontal response direction, while $T1_A$ represents the largest fundamental vibration period for the main horizontal response direction. To meet the requirements, the ratio between the target spectrum and the average spectrum of recorded earthquakes must be greater than 0.9. This research investigates the effects of including the complete interval (0s-15s) in the analysis to determine the scale factor. The purpose of this analysis is to assess if there is a statistically significant difference in the scale factor between the two intervals defined by SNI 8899:2020 when considering the entire period. The Firefly algorithm is employed to derive the scale factor by minimizing the limit ratio between the target spectrum and the average spectrum of recorded earthquakes. The scale factor derived from this method will be compared to the findings provided in SNI 8899:2020.

Firefly Algorithm

The firefly algorithm (FA) was initially introduced by [8] and is derived from the behavior of fireflies. The two key elements of FA are attraction and fluctuation in light intensity. The attractiveness of a firefly is determined by its luminosity, which is directly linked to the objective function. The basic formula in FA is used to calculate the motion of a firefly i that is drawn towards other fireflies. Equation (1) yields a more visually appealing (luminous) position for firefly j.

$$x_i^{t+1} = x_i^t + \beta_0 e^{-\gamma r_{ij}^2}\left(x_j^t - x_i^t\right) + \alpha\varepsilon_i^t \quad (1)$$

The second term, β_0, represents the attractiveness at zero distance (r=0). The term $e^{-\gamma r_{ij}^2}$ accounts for attractiveness. The third term, α, is the randomization parameter or mutation parameter. ε_i^t is a random vector number generated from either a Gaussian distribution or a uniform distribution at time *t*.

The FA algorithm is unique because it integrates the capabilities of three distinct optimization methods: Differential Evolution (DE), Simulated Annealing (SA), and Accelerated Particle Swarm Optimization (APSO). The representation of this ability can be found in equation (1). When the values of α and β are set to 0, the FA will transform into DE. When the value of β_0 is equal to zero, the FA becomes equivalent to the SA. When the variable x_i^t is substituted with the value of g*, the FA becomes equivalent to APSO. Thus, FA combines the advantages of Genetic Algorithm (GA) and Particle Swarm Optimization (PSO) and has proven to be more versatile and effective, surpassing these other methods [9].

METHODS

The Firefly Algorithm is employed to acquire scale coefficients for every earthquake record. The objective function used is to minimize the ratio between the average spectral acceleration of the considered earthquake recordings and the target spectrum, to reach the set limit value of 0.9. The mathematical expression for the objective function may be observed in equation (2). The fitness value is a numerical representation of the function of objectives that is to be minimized.

$$fitness = \frac{average\ spectral\ acceleration}{target\ response\ spectrum} \quad (2)$$

In addition, the scale coefficient is attempted not to exceed 5 [10]. When scaling based on SNI 1726:2019, two-period intervals are considered: $0.2T1_B$ - $2T1_A$ and $0.2T1_B$ - $1.5T1_A$. The study utilized eleven seismic recordings obtained from SNI 8899-2020, which describes the protocols for selecting and modifying surface ground motion. Appendix A of SNI 8899:2020 contains all the other parameters that were utilized. Table 1 shows the earthquake recordings used along with the magnitude of the earthquake recordings and the source of the earthquake recording data collected.

The target spectrum utilized is the spectrum response obtained from Jakarta city, Indonesia. Figure 1 is a flowchart illustrating the process of getting a scale factor using the amplitude scaling method with the firefly algorithm.

TABLE 1. The earthquake recordings used are based on Appendix A of the SNI 8899:2020.

Event	Years	Station	Magnitude	Source of Ground Motion Data
Muroran, Japan	1968	HK003	8.2	https://www.risksciences.ucla.edu/nhr3/nga-subduction/gmportal [11]
Taiwan	1986	SMART1 101	7.3	https://ngawest2.berkeley.edu/ [12]
Landers, USA	1992	Compton – Castlegate St	7.28	https://ngawest2.berkeley.edu/ [12]
Hector Mine, USA	1999	Indio – Riverside Co Fair Grnds	7.13	https://ngawest2.berkeley.edu/ [12]
Kocaeli, Turkey	1999	Hava Alani	7.51	https://ngawest2.berkeley.edu/ [12]
Chi-Chi, Taiwan	1999	CHY067	7.62	https://ngawest2.berkeley.edu/ [12]
Tokachi-Oki, Japan	2003	HKD083-Tsurui	8.3	https://www.kyoshin.bosai.go.jp/ [13]
Tokachi-Oki, Japan	2003	HKD094-Shihoro	8.3	https://www.kyoshin.bosai.go.jp/ [13]
Tohoku, Japan	2011	CHB008-Urayas	9	https://www.kyoshin.bosai.go.jp/ [13]
Tohoku, Japan	2011	KNG007-Fujisawa	9	https://www.kyoshin.bosai.go.jp/ [13]
Tohoku, Japan	2011	FKS021-Kitakata	9	https://www.kyoshin.bosai.go.jp/ [13]

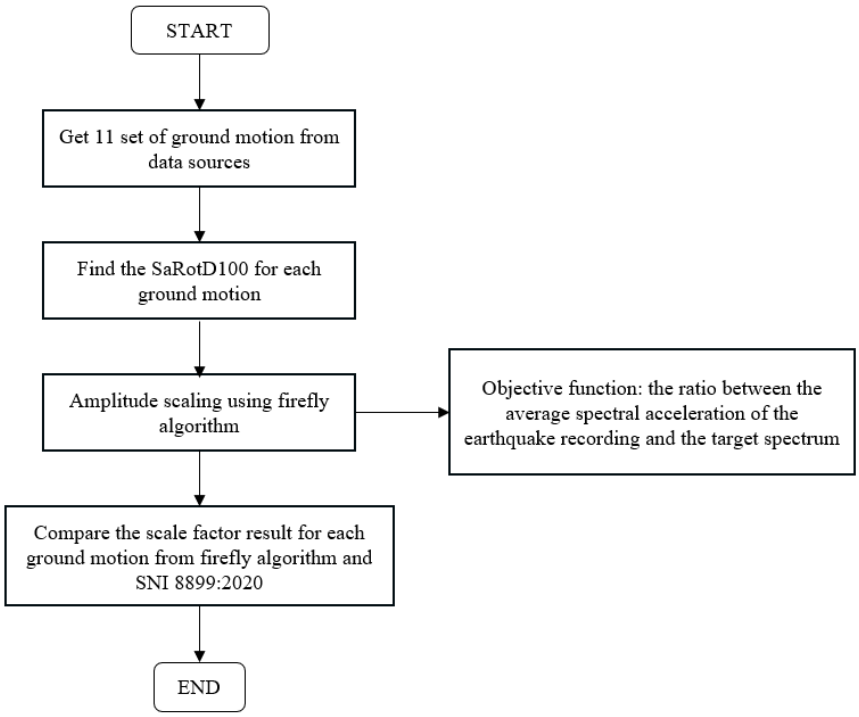

FIGURE 1. Flowchart for amplitude scaling for ground motion modification.

RESULT AND DISCUSSIONS

SaRotD100

According to SNI 8899:2020, the response spectrum utilized is the spectral acceleration response spectrum with the angular orientation that generates the highest response (SaRotD100). However, not all the reference sources listed in Table 1 provide the value of SaRotD100. Consequently, it is necessary to do an initial calculation to obtain the SaRotD100 value. An interface application program (Figure 2) was developed to transform the acceleration spectra acquired from a reference source using the *appdesigner* function provided by MATLAB [14,15]. A validation process was conducted to compare the findings obtained from the program developed with the reference source [11], which supplies SaRotD100 values. As an illustration, a single earthquake recording, specifically Tohoku-FKS021, is used to obtain the SaRotD100 value.

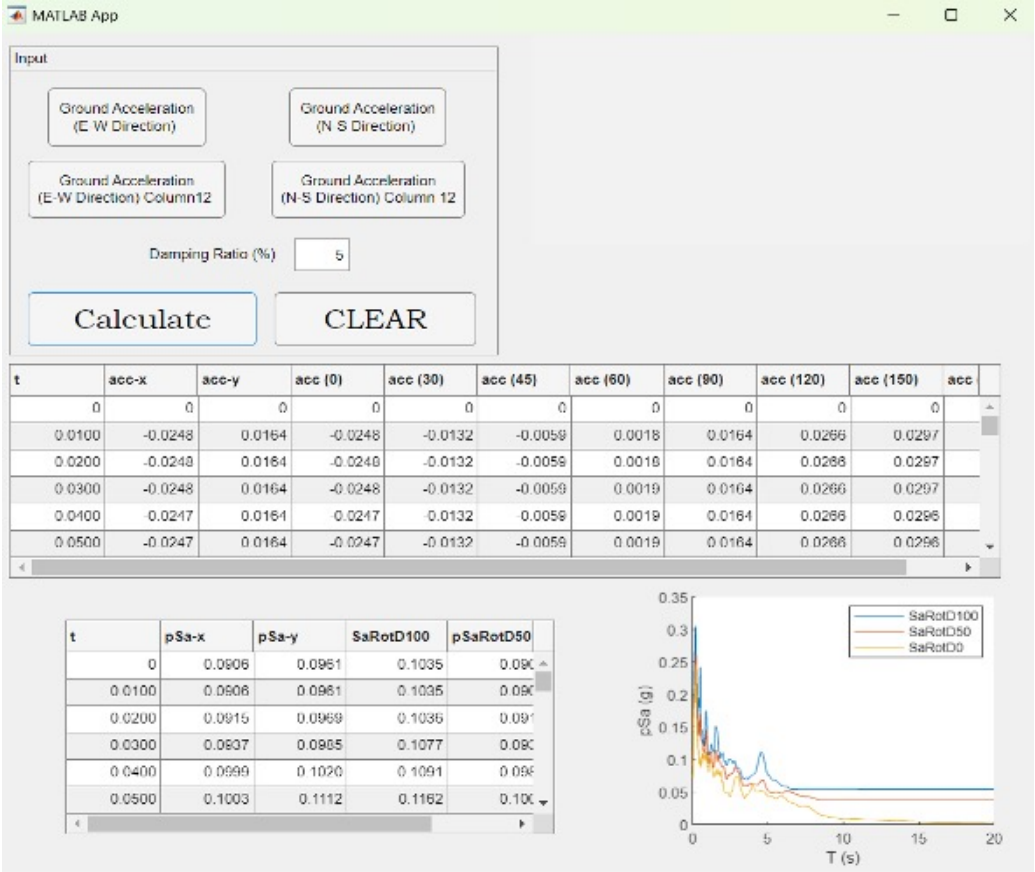

FIGURE 2. The interface application is used to obtain SaRotD100 values.

Figure 3 illustrates the correlation between pseudo spectral acceleration and time for the SaRotD100 parameter. The orange line represents the pseudo spectral acceleration findings obtained directly from [11], whereas the blue line represents the results obtained via the interface application program developed.

Tables 2 and 3 display the difference in pseudo acceleration derived from [11] within the time range of t = 0.01s –15s. The mean deviation is 2.8675%. From this, it can be inferred that there is no substantial difference between the data obtained from the website [11] and the data derived from the interface application to determine the SaRot100D value. Consequently, it can be concluded that the data from the interface application is suitable for subsequent analysis, specifically the amplitude scaling procedure.

Amplitude Scaling Using Firefly Algorithms

Figure 4 and Figure 5 display the ratio achieved through scaling for the period intervals ranging from $0.2T1_B$ – $2T1_A$ and from $0.2T1_B$ – $1.5T1_A$, respectively. The computed ratio value closely approximates the specified limit of 0.9 within the specified period. Nevertheless, the scale coefficient value derived from many earthquake records surpasses 5. Despite multiple attempts at additional optimization, no convergent solution has been found that can offer a scale coefficient of 5 or less. Furthermore, this aligns with the scale factor specified in SNI 8899:2020, as there are a few earthquake records with a magnitude greater than 5. This mostly results from the lack of earthquake events that exhibit the required seismic mechanism. Table 4 presents a comparison of the scaling outcomes achieved by the utilization of the Firefly Algorithm and the scaling specified in SNI 8899:2020.

TABLE 2. The difference in pSa values acquired from Peer Berkeley and Analysis during the time interval of t=0.01s to 0.9s.

t	pSa		Difference (%)	t	pSa		Difference (%)
	Peer Berkeley	Analysis			Peer Berkeley	Analysis	
0.01	0.0650	0.0652	0.2192	0.16	0.1373	0.1318	4.0014
0.02	0.0658	0.0662	0.6214	0.17	0.1363	0.1609	17.9835
0.022	0.0662	0.0666	0.6636	0.18	0.1728	0.1594	7.7601
0.025	0.0666	0.0668	0.2281	0.19	0.1484	0.1448	2.4191
0.029	0.0669	0.0663	0.9631	0.2	0.1573	0.1677	6.6101
0.03	0.0670	0.0664	0.9150	0.22	0.1429	0.1232	13.7795
0.032	0.0675	0.0668	1.0521	0.24	0.1253	0.1335	6.5818
0.035	0.0666	0.0677	1.5907	0.25	0.1442	0.1519	5.3127
0.036	0.0666	0.0680	2.0720	0.26	0.1506	0.1427	5.2459
0.04	0.0673	0.0691	2.7178	0.28	0.1429	0.1360	4.8338
0.042	0.0677	0.0679	0.3125	0.29	0.1376	0.1324	3.7849
0.044	0.0687	0.0667	2.9620	0.3	0.1278	0.1145	10.3989
0.045	0.0690	0.0674	2.3342	0.32	0.1374	0.1416	3.0386
0.046	0.0693	0.0680	1.8740	0.34	0.1452	0.1401	3.5183
0.048	0.0695	0.0694	0.1147	0.35	0.1367	0.1299	4.9426
0.05	0.0684	0.0691	1.1291	0.36	0.1249	0.1177	5.7916
0.055	0.0698	0.0668	4.2668	0.38	0.1022	0.1045	2.2281
0.06	0.0692	0.0695	0.4615	0.4	0.1101	0.1174	6.7045
0.065	0.0663	0.0764	15.2948	0.42	0.1293	0.1307	1.0799
0.067	0.0703	0.0781	10.9712	0.44	0.1339	0.1333	0.4641
0.07	0.0750	0.0802	6.9048	0.45	0.1329	0.1315	1.0882
0.075	0.0791	0.0814	2.9084	0.46	0.1324	0.1363	3.0169
0.08	0.0807	0.0855	5.9694	0.48	0.1559	0.1621	3.9829
0.085	0.0844	0.0836	0.9774	0.5	0.1848	0.1953	5.6327
0.09	0.0834	0.0901	7.9831	0.55	0.2386	0.2380	0.2541
0.095	0.0878	0.1005	14.3911	0.6	0.2110	0.2029	3.8597
0.1	0.1014	0.0993	2.1342	0.65	0.1812	0.1846	1.8716
0.11	0.0966	0.0991	2.6343	0.667	0.1941	0.1975	1.7569
0.12	0.1027	0.0998	2.8681	0.7	0.1947	0.1897	2.5538
0.13	0.1095	0.1243	13.5226	0.75	0.1329	0.1334	0.3668
0.133	0.1179	0.1307	10.8813	0.8	0.1193	0.1192	0.0958
0.14	0.1315	0.1472	11.8932	0.85	0.1143	0.1142	0.1425
0.15	0.1415	0.1340	5.3071	0.9	0.1120	0.1109	0.9764

TABLE 3. The difference in pSa values acquired from Peer Berkeley and Analysis during the time interval of t=0.95s to 15s.

t	pSa		Difference (%)	t	pSa		Difference (%)
	Peer Berkeley	Analysis			Peer Berkeley	Analysis	
0.95	0.1142	0.1142	0.0221	4	0.0319	0.0317	0.7781
1	0.1213	0.1213	0.0544	4.2	0.0318	0.0315	0.7370
1.1	0.1363	0.1373	0.7213	4.4	0.0307	0.0306	0.3153
1.2	0.1203	0.1220	1.3993	4.6	0.0346	0.0340	1.6187
1.3	0.1388	0.1390	0.1781	4.8	0.0381	0.0381	0.0893
1.4	0.1371	0.1327	3.2156	5	0.0360	0.0361	0.1252
1.5	0.1270	0.1256	1.0883	5.5	0.0337	0.0339	0.5872
1.6	0.1121	0.1112	0.7769	6	0.0297	0.0296	0.1977
1.7	0.1176	0.1167	0.7583	6.5	0.0259	0.0260	0.2239
1.8	0.1046	0.1019	2.6279	7	0.0245	0.0241	1.6240
1.9	0.0912	0.0917	0.5373	7.5	0.0222	0.0222	0.3899
2	0.0961	0.0964	0.3874	8	0.0188	0.0188	0.2506
2.2	0.0974	0.0964	0.9832	8.5	0.0188	0.0189	0.3572
2.4	0.0664	0.0643	3.2028	9	0.0187	0.0188	0.4636
2.5	0.0574	0.0577	0.5785	9.5	0.0176	0.0176	0.0772
2.6	0.0569	0.0567	0.5119	10	0.0136	0.0133	2.1908
2.8	0.0536	0.0536	0.0296	11	0.0079	0.0079	0.0140
3	0.0585	0.0577	1.2417	12	0.0074	0.0074	0.1677
3.2	0.0507	0.0504	0.6296	13	0.0070	0.0070	1.2018
3.4	0.0493	0.0493	0.1033	14	0.0058	0.0059	1.0962
3.5	0.0495	0.0496	0.2325	15	0.0048	0.0047	1.2014
3.6	0.0474	0.0474	0.0813		Average		2.8675
3.8	0.0385	0.0380	1.1420				

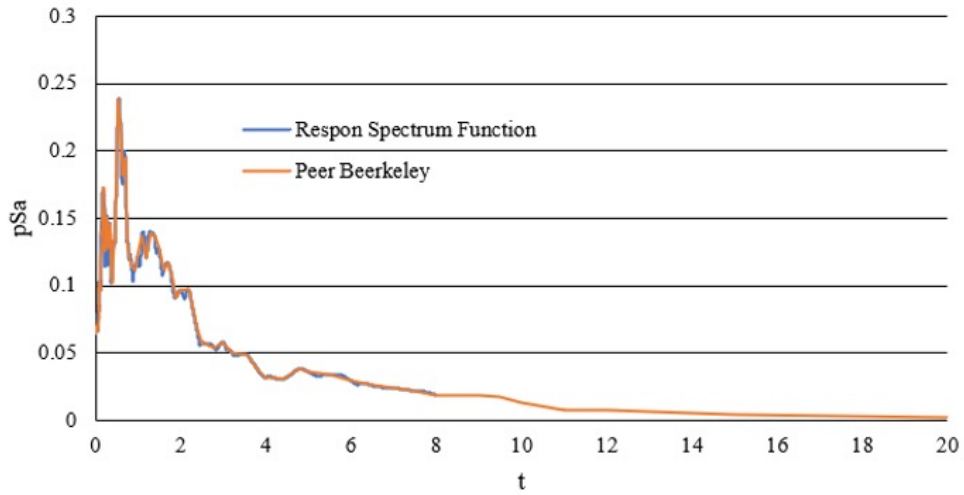

FIGURE 3. Relationship between t-pSa (Interface Application vs Peer Beerkeley) for SaRot100D (ChiChi-CHY067).

TABLE 4. Comparison of scaling results.

Event (Station)	Scaled Factor (Result)		Scaled Factor (SNI 8899:2020)	
	$0.2T_1B$-$2T_1A$	**$0.2T_1B$-$1.5T_1A$**	**$0.2T_1B$-$2T_1A$**	**$0.2T_1B$-$1.5T_1A$**
Taiwan (SMART1 101)	2.8044	2.1112	4.45	3.21
Landers, USA (Compton – Castlegate St)	2.8041	2.6112	4.39	4.2
Hector Mine, USA (Indio – Riverside Co Fair Grnds)	3.1553	1.9366	4.27	3.36
Kocaeli, Turkey (Hava Alani)	5.4500	6.0273	4.99	4.23
Chi-Chi, Taiwan (CHY067)	3.2483	1.0000	7.09	6.06
Tokachi-Oki, Japan (HKD083-Tsurui)	1.0000	1.0000	3.00	2.29
Tokachi-Oki, Japan (HKD094-Shihoro)	3.3041	4.0983	4.70	3.62
Tohoku, Japan (CHB008-Urayas)	5.3293	6.0112	3.13	2.53
Tohoku, Japan (KNG007-Fujisawa)	1.9055	2.2277	6.12	4.86
Tohoku, Japan (FKS021-Kitakata)	1.1676	1.0362	5.11	4.15
Muroran, Japan (HK003)	5.1002	6.0153	5.54	4.77

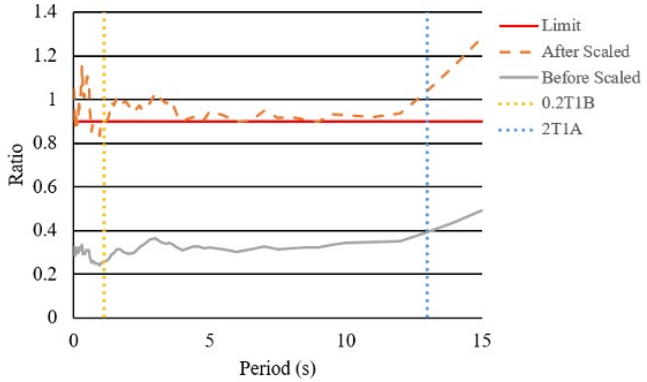

FIGURE 4. The ratio of the average spectral acceleration of earthquake recordings to the target acceleration spectrum for the period interval $0.2T1_B$ - $2T1_A$.

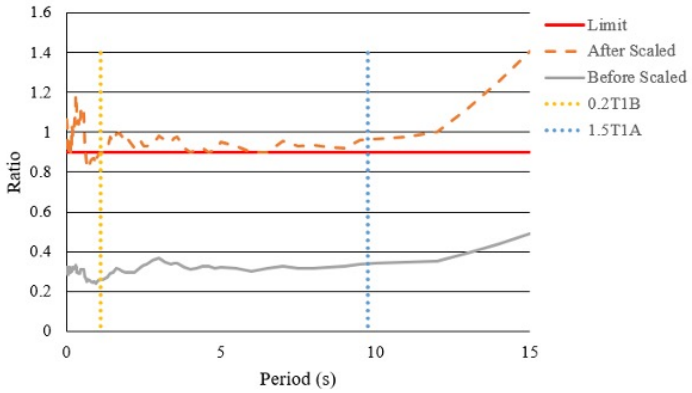

FIGURE 5. The ratio of the average spectral acceleration of earthquake recordings to the target acceleration spectrum for the period interval $0.2T1_B$ – $1.5T1_A$.

Figure 6 and Figure 7 depict the scaled spectral acceleration for each earthquake recording used, specifically for the periods ranging from $0.2T1_B$ - $2T1_A$ and $0.2T1_B$ – 1.5T1A, respectively.

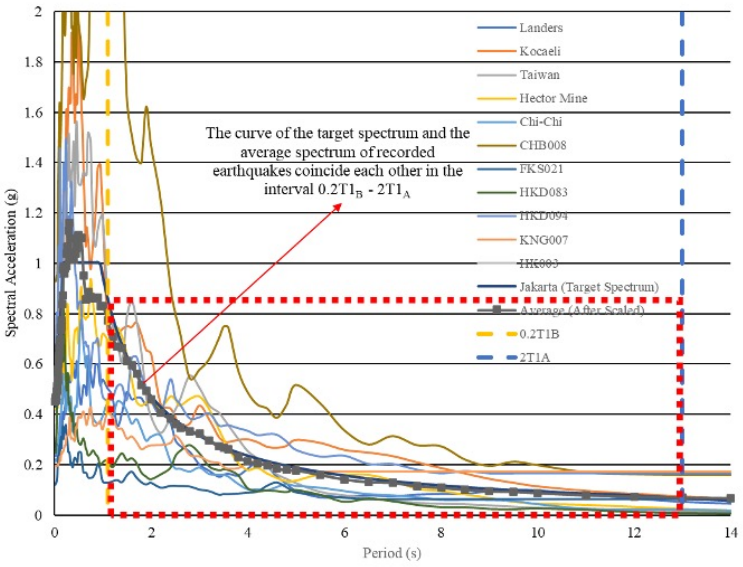

FIGURE 6. Results of acceleration spectral scaling for all earthquake records used between $0.2T1_B$ - $2T1_A$.

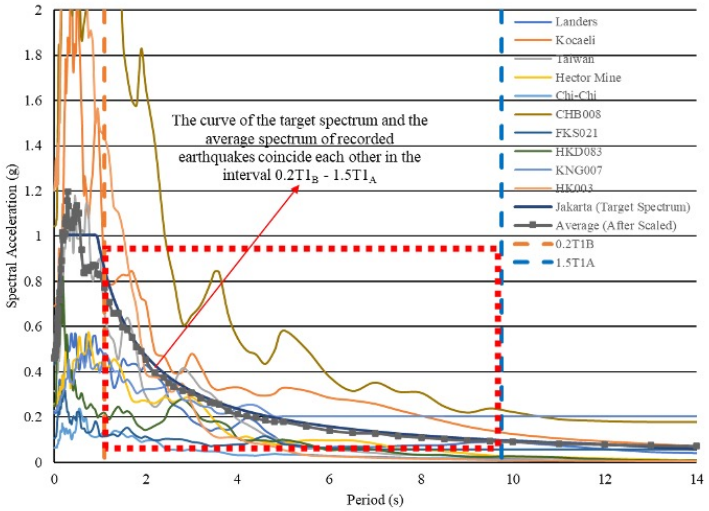

FIGURE 7. Results of acceleration spectral scaling for all earthquake records used between $0.2T1_B$ - $1.5T1_A$.

It is noticeable that following the 0.2T1B period, the average spectral acceleration of the earthquake recordings closely matches the target spectrum acceleration for both period intervals. This result demonstrates that the current results are less cautious than those obtained in SNI 8899:2020. In SNI 8899:2020, the scale coefficient produced an average spectral acceleration value for earthquake recordings that exceeded around 30% of the target acceleration spectrum.

As shown in Figures 4 and 5, the scaling results result in a ratio value > 0.9 in the specified period ($0.2T1_B – 2T1_A$ and $0.2T1_B – 1.5T1_A$), but a ratio value < 0.9 in the period < $0.2T1_B$. This is so because optimizations are only done within the specified interval range—it never occurs more than it. As a result, a test was run to determine the scale factor by entering the whole period (0s-15s). The scaling results are shown in Figure 8 and Table 5 for the full period of 0 s to 15 s. No ratio value is less than 0.9, but the highest coefficient value of the scale factor that can be obtained is 6.6422, indicating that the scale factor is larger than the coefficient of this scale factor. obtained between $0.2T1_B – 2T1_A$ and $0.2T1_B – 1.5T1_A$ interval intervals. The period of the average spectral acceleration value of earthquake recordings and the target acceleration spectrum, as shown in Figure 9, do not significantly differ according to the comparison results of the response spectrum produced. The comparison results (period scaling $0.2T1_B – 2T1_A$ and $0.2T1_B – 1.5T1_A$) continue the previous trend.

TABLE 5. Scale factor obtained for interval period 0s – 15s.

Event (Station)	Scaled Factor
Taiwan (SMART1 101)	4.1075
Landers, USA (Compton – Castlegate St)	2.1304
Hector Mine, USA (Indio – Riverside Co Fair Grnds)	1.5696
Kocaeli, Turkey (Hava Alani)	6.6422
Chi-Chi, Taiwan (CHY067)	4.5168
Tokachi-Oki, Japan (HKD083-Tsurui)	1.2656
Tokachi-Oki, Japan (HKD094-Shihoro)	2.4541
Tohoku, Japan (CHB008-Urayas)	6.4193
Tohoku, Japan (KNG007-Fujisawa)	1.6391
Tohoku, Japan (FKS021-Kitakata)	1.2709
Muroran, Japan (HK003)	4.4086

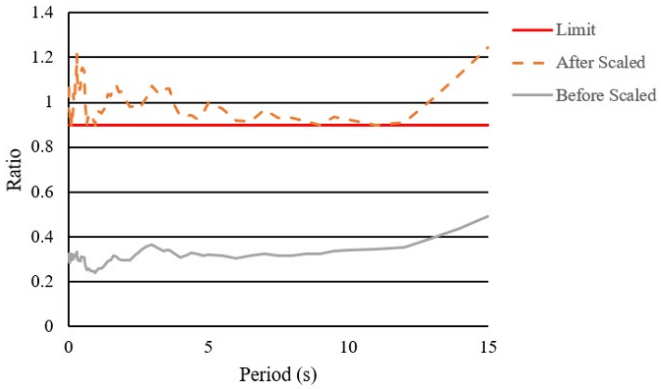

FIGURE 8. The ratio of the average spectral acceleration of earthquake recordings to the target acceleration spectrum for the period interval 0s-15s.

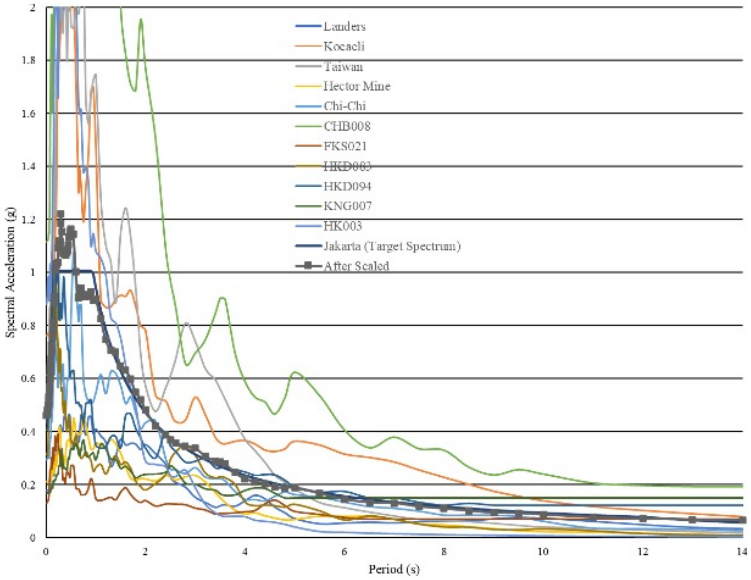

FIGURE 9. Results of acceleration spectral scaling for all earthquake records used between 0s – 15s.

CONCLUSION

This study aims to determine a scale factor that is not excessively conservative using the Firefly Algorithm. This will be achieved by reducing the ratio between the target spectrum and the average spectrum of recorded earthquakes. The goal is made to ensure that this ratio closely approximates the suggested value of 0.9. A total of 11 seismic recordings have been used for analysis. The earthquake recording was sourced straight from Appendix A in SNI 8899:2020. The scale factor derived via SNI 8899:2020 is contrasted with the scale factor acquired through the utilization of the firefly method. The results indicate that the firefly algorithm's scale factor produces an earthquake-recording spectrum response curve that closely matches the target spectrum response curve within a specific range (0.2T1B – 2T1A and 0.2T1B – 1.5T1A), better than the scale factor shown in SNI 8899:2020. This result suggests that the scale factor is less conservative when compared to the scale factor in SNI 8899:2020.

REFERENCES

1. M. Palanci, A. Demir and A.H. Kayhan, "Quantifying the effect of amplitude scaling of real ground motions based on structural responses of vertically irregular and regular RC frames", Structures **51**, 105-123 (2023).
2. Standardization Agency of Indonesia (BSN). “Persyaratan beton struktural untuk bangunan gedung dan penjelasan”, SNI 1726:2019 (BSN, Jakarta, 2019).
3. Standardization Agency of Indonesia (BSN). “Tata cara pemilihan dan modifikasi gerak tanah permukaan untuk perencanaan gedung tahan gempa”, SNI 8899:2020 (BSN, Jakarta, 2020).
4. Y. A. Heo, S. K. Kunnath and N. Abrahamson. "Amplitude-scaled versus spectrum-matched ground motions for seismic performance assessment", J.Struct.Eng **137** (3), 278-288 (2011).
5. E. Cavdar, G. Ozdemir and B. Bayhan, "Significance of ground motion scaling parameters on amplitude of scale factors and seismic response of short- and long-period structures", Earthquake Spectra **35**(4), 1663-1688 (2019).
6. J. Fayaz, P. T. Rodas, M. Medalla and F. Naeim, "Assessment of ground motion amplitude scaling using interpretable Gaussian process regression: application to steel moment frames", Earthquake Engineering & Structural Dynamics **52**, 2339-2359 (2023).
7. A. Kurniawandy, M. Aminsyah, B.V. Cahyadi and Z. Djauhari, "Comparative study of the simulation ground motion by amplitude scale and spectral matching" in *The Second International Conference on Disaster Mitigation and Management-2023*. E3S Web of Conferences 464 (2023).
8. X. S. Yang, "Nature-inspired metaheuristic algorithm. 2nd edition," Luniver Press, United Kingdom, 2010.
9. X.S. Yang," Nature-inspired optimization algorithm. 1st edition," Elsevier, London, 2014.
10. F. Zareian and P. Zhong, "Ground motion selection and scaling for the analysis of the tall building case studies. PEER, 2010.
11. The B. John Garrick Institute, https://www.risksciences.ucla.edu/nhr3/nga-subduction/gmportal, accessed on February, 2024.
12. Pacific Earthquake Engineering Research Center, https://ngawest2.berkeley.edu, accessed on November, 2023.
13. National Research Institute for Earth Science and Disaster Resilience, https://www.kyoshin.bosai.go.jp/, accessed on November, 2023.
14. MathWorks, "MATLAB: Primer, Version 8.6. The Mathworks, Inc.", 2015.
15. MathWorks, "MATLAB: Programming Fundamental, Version 8.6. The Mathworks, Inc.", 2015.